# Selective Hydrogenation of Citral over a Carbon-titania Composite Supported Palladium Catalyst

Zhu, Jie(朱劼)　Lu, Mohong(鲁墨弘)　Li, Mingshi*(李明时)
Zhu, Jianjun(朱建军)　Shan, Yuhua(单玉华)

*School of Petrochemical Engineering, Changzhou University, Changzhou, Jiangsu 213164, China*

A novel carbon-titania composite material, $C/TiO_2$, has been prepared by growing carbon nanofibers (CNFs) on $TiO_2$ surface via methane decomposition using Ni-Cu as a catalyst. The $C/TiO_2$ was used for preparing supported palladium catalyst, $Pd/C/TiO_2$. The support and $Pd/C/TiO_2$ catalyst were characterized by BET, SEM, XRD and TG-DTG. Its catalytic performance was evaluated in selective hydrogenation of citral to citronellal, and compared with that of activated carbon supported Pd catalyst. It was found that the $Pd/C/TiO_2$ catalyst contains 97% of mesopores. And it exhibited 88% of selectivity to citronellal at citral conversion of 90% in citral hydrogenation, which was much higher than that of activated carbon supported Pd catalyst. This result may be attributed to elimination of internal diffusion limitations, which were significant in activated carbon supported Pd catalyst, due to its microporous structure.

**Keywords** carbon-titania composite, carbon nanofibers, hydrogenation, citral, internal diffusion

## Introduction

Citral, a typical $\alpha,\beta$-unsaturated aldehydes, is important in fine chemical and pharmaceutical industries in that there are three sites of hydrogenation: a conjugate double bond (C=C), a carbonyl group (C=O) and an isolated double bond (C=C). The reduction of citral would lead to a consecutive reaction network (Figure 1). Citronellal, an intermediate product of the consecutive reactions, can be hydrogenated easily to citronellol and finally to 3,7-dimethyloctan-1-ol.[1-4] Several systematic studies on citral selective hydrogenation have been reported. These studies covered almost all important aspects such as active metals including mono-catalysts[2,5-11] and the roles of catalyst supports.[12-15] Specifically, Yilmaz *et al.*[12] reported the highest selectivity (90%) to citronellal so far, at complete conversion of citral over Pd/natural zeolite, which was explained by the active metal properties and the absence of significant internal diffusion limitations.

Titania and their composites have usually been focused on the study of photocatalytic properties.[16,17] While in this work, we prepared carbon-titania composite as a novel catalyst support, named $C/TiO_2$. The prepared $C/TiO_2$ and its supported palladium catalyst, $Pd/C/TiO_2$, have been characterized using various methods. Meanwhile, the catalytic performance of the $Pd/C/TiO_2$ catalyst has been evaluated in selective hydrogenation of citral to citronellal, and compared with a commercial catalyst, *i.e.*, activated carbon supported palladium.

## Experimental

### Preparation of $C/TiO_2$ composite

The cylindrical $TiO_2$ (Sinopec Yangzi, China, $\varphi 2\times 6$ mm; 18.2 $m^2\cdot g^{-1}$) was used in this study to prepare $C/TiO_2$ composite material. Specifically, $C/TiO_2$ was prepared by impregnation of $TiO_2$ with aqueous solution of $Ni(NO_3)_2\cdot 6H_2O$ and $Cu(NO_3)_2\cdot 3H_2O$ (A.R., Sinopharm, China), in which the nickel loading was fixed at 6 wt% while the molar ratio of Ni to Cu was 8 to 1.[18] Then, the samples were dried overnight at 393 K prior to calcination in muffle furnace at 773 K for 2 h. The samples were subsequently loaded inside a quartz tube and reduced at 873 K in a gas mixture of $N_2$ and $H_2$ (99.999%, Wuxi Tianhong, China) for 3 h. Methane (99.999%, Wuxi Tianhong, China) was passed through the tube to decompose at 873 K for 5 h. After being cooled down to the room temperature under $N_2$ protection, the composite support $C/TiO_2$ was obtained. Finally, the exposed nickel and copper metal particles were removed by stirring the composite in concentrated $HNO_3$ for 2 h.

### Preparation of $C/TiO_2$ supported Pd catalyst

0.5 wt% of Pd catalyst was prepared via chemical reduction process. Firstly, ethylenediaminetetraacetic

---

* E-mail: mingshili@yahoo.com; Tel.: 0086-0519-86330360; Fax: 0086-0519-86330360
Received September 14, 2010; revised December 17, 2010; accepted December 24, 2010.
Project supported by the National Natural Science Foundation of China (No. 20976076) and the Natural Science Foundation of Jiangsu Province (No. BK2009536).

© 2011 SIOC, CAS, Shanghai, & WILEY-VCH Verlag GmbH & Co. KGaA, Weinheim

acid (EDTA) solution (A.R., Sinopharm, China) was added dropwise into an aqueous solution of $PdCl_2$ (Pd≥59%, Sinopharm, China) and stirred for 3 h to obtain Pd-EDTA chelates. Secondly, the support was impregnated with Pd-EDTA chelates, and stirred continuously overnight. Then, the pH of the solution was adjusted to 9—10 and the catalyst was reduced at 363 K for 2 h using hydrazine hydrate. Finally, the reduced catalyst was collected via filtration followed by subsequent washing to remove $Cl^-$. The catalyst prepared was named Pd/C/$TiO_2$.

### Characterization of supports and catalysts

C/$TiO_2$ support and Pd/C/$TiO_2$ catalyst were characterized to test the textural and structural properties. X-ray powder diffraction data were collected on Rigaku D/max 2500 diffractometer using CuKα (40 kV, 40 mA) radiation and a graphite monochromator. The BET specific surface areas were carried out with Micromeritics ASAP 2010 apparatus. Scanning electron images were recorded using a JEOL JSM-6360 LA scanning electron microscope. Thermogravimetric (TGA) and differential thermal (DTA) analysis were performed using a TA SDT Q600 instrument.

### Activity test of Pd/C/$TiO_2$

The catalytic activity of Pd/C/$TiO_2$ has been evaluated in selective hydrogenation of citral in liquid phase. The reaction was conducted in a 100 mL autoclave at 363 K and 3 MPa. By dispersing the catalysts (1 wt%) into the isopropanol (A.R., Sinopharm, China) solution of citral (10 wt%, A.R., Sinopharm, China), the autoclave was sufficiently flushed with nitrogen flow to remove dissolved oxygen. The reaction pressure was maintained by injecting hydrogen. Small amounts of reaction samples were withdrawn from the reactor at different reaction times and analyzed by gas chromatography (VARIAN CP3800) equipped with a FID detector and a capillary column HP-5 using nitrogen as carrier gas. A formed activated carbon supported catalyst, named Pd/AC, (Pd loading 0.5 wt%, Sinopec Yangzi, China) was tested at the same conditions for comparison. In examining the influence of the structure of the catalyst on citral hydrogenation, we defined the citral conversion $X$ and the selectivity towards reaction products $S$ as

$$X=\frac{n^0_{\mathrm{Citral}}-n_{\mathrm{Citral}}}{n^0_{\mathrm{Citral}}}\times 100\% \tag{1}$$

$$S_i=\frac{n_i}{\sum n_i}\times 100\% \tag{2}$$

where $n$ is the temporal molar amount of the reactant or the product during citral hydrogenation; $n^0$ is the initial molar amount of the reactant; $i$ is the reaction product shown in Figure 1 including citronellal, citronellol, 3,7-dimethyloctanol, geraniol, nerol and isopulegol.

## Results and discussion

### Characterizations of the catalyst

**BET analysis** The novel C/$TiO_2$ composite can be produced by depositing carbon onto $TiO_2$ host by methane decomposition. The surface properties of such prepared C/$TiO_2$ composites were different from the corresponding $TiO_2$ hosts, as shown in Table 1. Specifi-

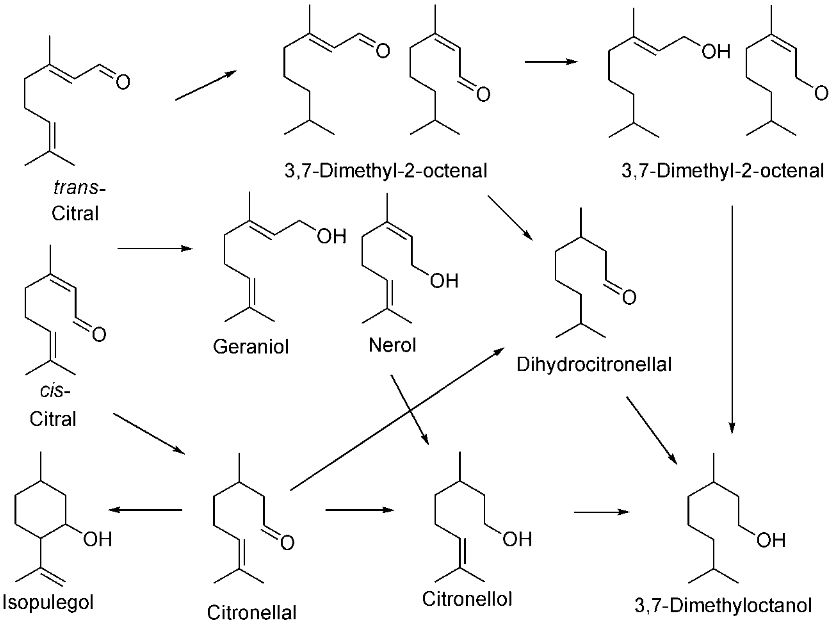

**Figure 1** The consecutive reaction network for citral hydrogenation.

© 2011 SIOC, CAS, Shanghai, & WILEY-VCH Verlag GmbH & Co. KGaA, Weinheim

**Table 1** Textural properties of the catalysts

| Sample | Weight increased after methane decomposition/wt% | BET surface area/ ($m^2$•$g^{-1}$) | Micropore area/ ($m^2$•$g^{-1}$) | Average pore diameter/nm |
|---|---|---|---|---|
| $TiO_2$ support | — | 18.3 | 3.1 | 14.2 |
| $C/TiO_2$ composite | 38 | 60.3 | 1.8 | 6.2 |
| $Pd/C/TiO_2$ catalyst | — | 58.1 | 1.6 | 9.7 |
| Pd/AC (commercial) catalyst | — | 810 | 720 | 2.1 |

cally, depositing carbon on $TiO_2$ hosts can cause a significant increase in BET surface area. The BET surface area of $C/TiO_2$ was 60 $m^2/g$, much larger than 18 $m^2/g$ of its $TiO_2$ host while its micropore area decreased significantly to 1.8 $m^2/g$, accounting for only 3% of its total BET surface area. In contrast, the micropore area of original $TiO_2$ accounted for 16.9% of its total BET surface area. Therefore, it can be inferred that some micropores in $TiO_2$ may be blocked due to the formation of carbon deposits, and this may decrease internal diffusion during multiphase catalytic reactions. It was noted that after Pd loading over $C/TiO_2$, the surface properties of the $Pd/C/TiO_2$ catalyst were similar to the $C/TiO_2$ support, which suggested that the preparation method of $Pd/C/TiO_2$ catalyst in this work would not damage the structure of the catalyst.

**SEM analysis** As shown by SEM images in Figure 2a, a significant amount of CNFs with diameters of 50—80 nm covered the surface of $TiO_2$. The thickness of the deposition layer identified from an SEM image of $C/TiO_2$ cross section in Figure 2b is about 1.5 μm. Particularly, some CNFs appeared even in the interior of the hosts.

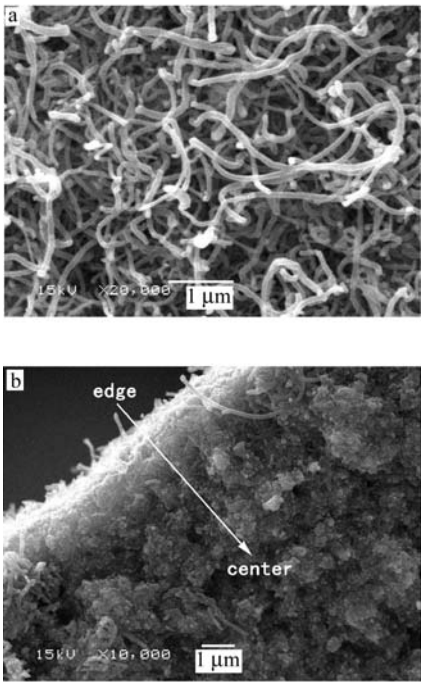

**Figure 2** SEM images of $C/TiO_2$ prepared by decomposition of methane over $Ni-Cu/TiO_2$: (a) the surface of $C/TiO_2$; (b) the cross section of $C/TiO_2$.

**TG-DTG analysis** Thermogravimetric analysis has been conducted to determine the percentage of carbon deposited into the catalyst as well as its structural properties. The results are shown in Figure 3.

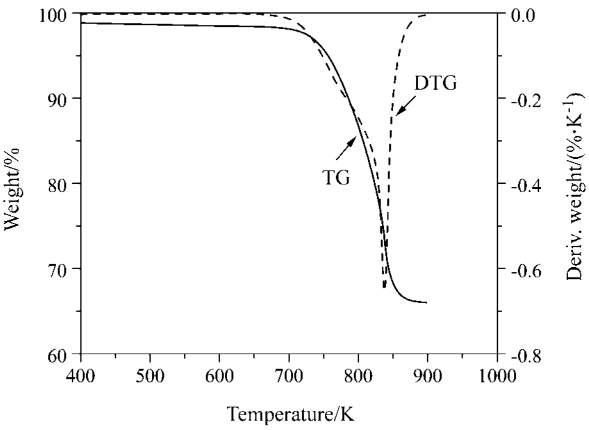

**Figure 3** TG and DTG curves of $Pd/C/TiO_2$ (Solid line corresponds TG curve; dashed line corresponds to DTG curve).

The total weight loss of $Pd/C/TiO_2$ catalyst in temperature range from 573 to 973 K was over 35%, as calculated from TG curve, being near to that of weight increase in the support (Table 1). Generally, amorphous carbon and graphite carbon have their own characteristic oxidation temperatures. A higher oxidation temperature always indicates a purer and less defective material. The oxidation temperature of amorphous carbon is relatively low, *i.e.*, in a range of 573 to 673 K, while that of graphite carbon is ranging from 673 to 973 K.[19] Therefore, the structure of carbon deposits can be well estimated from the DTG curve. Particularly, it can be inferred from the TG curve in Figure 3 that over 95% weight loss occurred between 673 and 973 K with the DTG peak at 853 K while only a little weight loss occurred between 573 and 673 K. Therefore, it is reasonable to conclude that about 95% carbon deposits produced by methane decomposition are graphite. It should be noted that CNFs have graphite structure.[17] However, the CNF structure in the interior of $C/TiO_2$ was not clearly observed by using SEM (Figure 2b) probably because CNF structure might be covered by a small percentage of amorphous carbon. Therefore, we supposed that the graphite in the interior of $Pd/C/TiO_2$ was mainly CNFs.

**XRD analysis** The structure of $Pd/C/TiO_2$ has been further analyzed using XRD. The XRD spectrum is shown in Figure 4, in which the characteristic peaks of graphite (002) and graphite (101) at 2*θ* (26.38°, 44.39°) were clearly evident, indicating the dominance of graphite carbon deposit in host material after methane decomposition. However, the characteristic palladium crystal peaks at 2*θ* (40.1°, 46.6°, 68.1°, 82.1°, 86.6°) were not obvious. It was supposed that the low Pd loading (0.5 wt%) may result in small Pd crystal, which cannot be measured by XRD.

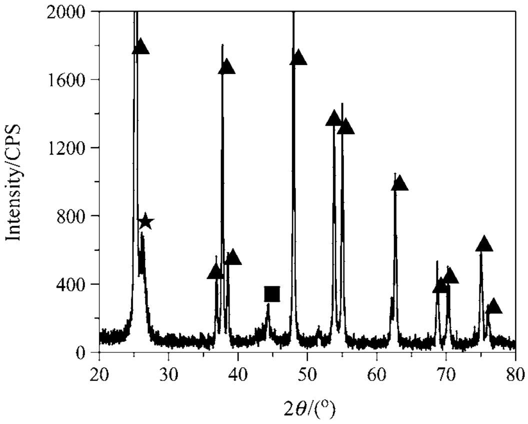

**Figure 4** XRD pattern of Pd/C/$TiO_2$: ▲ Anatase-$TiO_2$; ★ graphite (002); ■ graphite (101).

In summary, during methane decomposition, a significant amount of carbon was deposited on the surface of $TiO_2$ host, among which nearly 95% were CNFs. The external surface of the host was covered by a thick CNFs layer, while internal pores were filled mostly with CNFs along with a small percentage of amorphous carbon, which cannot be identified using SEM. Comparing to $TiO_2$ host, the BET surface area of C/$TiO_2$ increased greatly after carbon depositing. Furthermore, the decline in micropore area will lower the internal diffusion during multiphase catalytic reactions.

## Evaluation of Pd/C/$TiO_2$ catalytic activity

The catalytic performance of C/$TiO_2$ supported Pd catalyst (Pd/C/$TiO_2$) in hydrogenation of citral was evaluated and the results were compared with those of commercial Pd catalyst Pd/AC (Figures 5, 6). As shown in Figure 5, the catalytic activity of Pd/C/$TiO_2$ was much lower than that of Pd/AC. For example, the citral conversion over Pd/AC was 90% after 4 h, while it took 32 h for Pd/C/$TiO_2$ catalyst to reach the same conversion. The relatively low activity of Pd/C/$TiO_2$ might be due to the low specific surface area of the catalyst (Table 1). However, the major products over Pd/AC were citronellal and 3,7-dimethyloctanol, while citronellal over Pd/C/$TiO_2$, as shown in Figure 6a and 6b. The citronellal selectivity of Pd/C/$TiO_2$ was significantly higher than that of commercial Pd/AC. Particularly, at the citral conversion 90%, the selectivity of Pd/C/$TiO_2$ can be as high as 88%, being much higher than that of Pd/AC, 35%. The difference in selectivity between Pd/C/$TiO_2$ and Pd/AC is very likely due to the difference of the catalyst structures. Pd/C/$TiO_2$ mainly consists of mesopores and the micropore area only accounts for 3% of its total BET surface area, compared with Pd/AC (89%) according to Table 1.

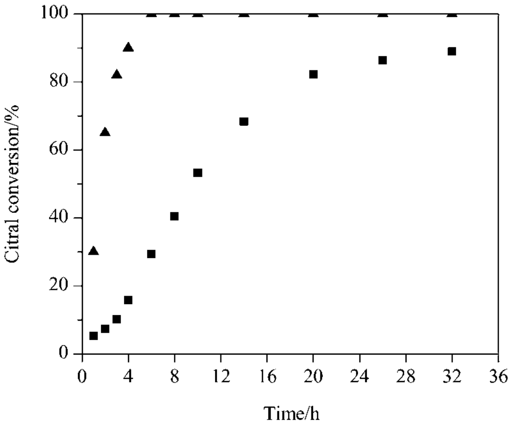

**Figure 5** Citral conversion versus reaction time in citral hydrogenation at 363 K and 3 MPa over Pd/C/$TiO_2$ (■) and commercial Pd/AC (▲).

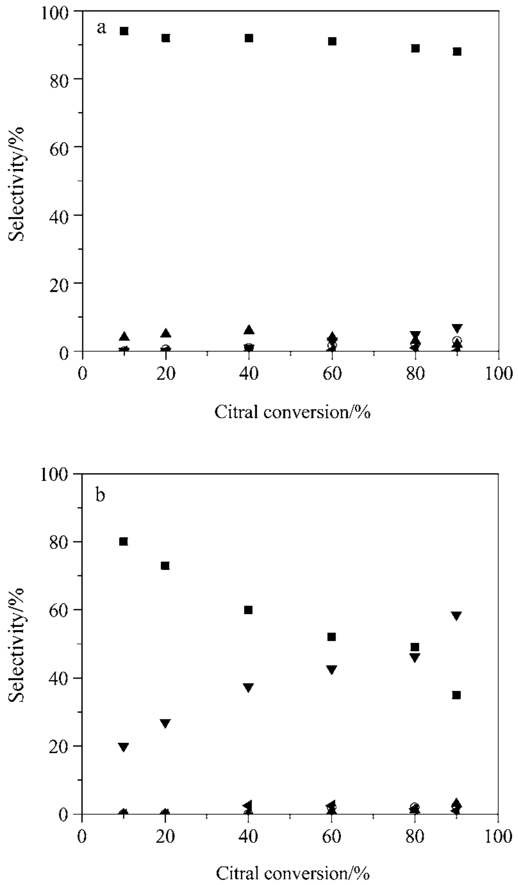

**Figure 6** The product distribution versus citral conversion in citral hydrogenation at 363 K and 3 MPa over Pd/C/$TiO_2$ (a) and commercial Pd/AC (b): ■ Citronellal; ▲ citronellol; ▼ 3,7-dimethyloctanol; ◀ geraniol+nerol; ○ isopulegol.

© 2011 SIOC, CAS, Shanghai, & WILEY-VCH Verlag GmbH & Co. KGaA, Weinheim

Palladium catalysts are very active in the hydrogenation of the C=C bond.[20] Therefore, citral was firstly hydrogenated to citronellal on external surface of the catalyst (Figure 7a), and then citronellal is easily desorbed from Pd crystal to the solution. When citral diffused from external surface to different pores of the catalyst, it hydrogenates to different products. If the reaction took place in the macro- and mesopore (Figure 7b) of the catalyst, the intermediate product, citronellal, easily desorbed to the solution, as the same on external surface of the catalyst. However, if the reaction took place inside the micropore, citronellal was confined in it long enough to be further hydrogenated to 3,7-dimethyloctanol (Figure 7c) due to the limitation of the internal diffusion.

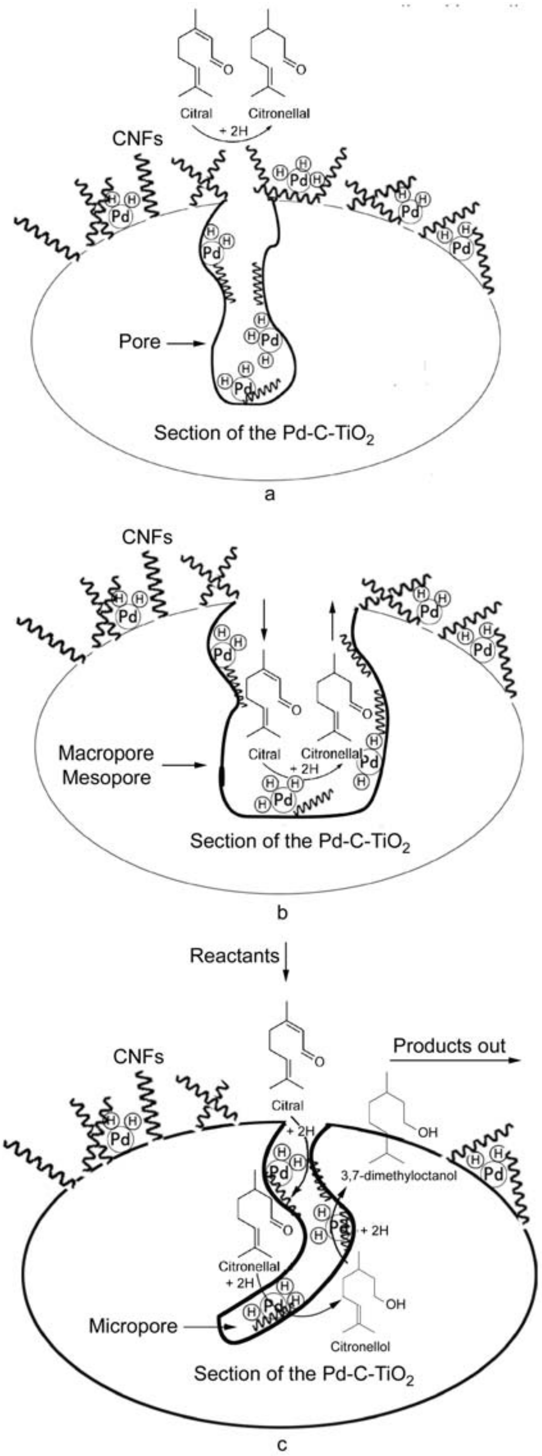

**Figure 7** The process of citral hydrogenation over Pd/C/$TiO_2$: (a) on external surface of the catalyst; (b) in the macro- and mesopores; (c) in the micropores.

It was noted that during the initial reaction over Pd/AC with citral conversion less than 10%, the selectivity to citronellal was comparatively high (80%) (Figure 6b). This was attributed to the citral hydrogenation on external surface of Pd/AC. With the reaction going on, citral was deeply hydrogenated to 3,7-dimethyloctanol on internal surface of Pd/AC due to its high micropore area. Therefore, the selectivity to citronellal decreases rapidly with the increase of citral conversion (Figure 6b). However, the influence of internal diffusion limitation on Pd/C/$TiO_2$ was not significant since Pd/C/$TiO_2$ had much fewer micropores than Pd/AC. Therefore, the selectivity to citronellal was almost constant with the increase of citral conversion over Pd/C/$TiO_2$ (Figure 6a).

## Conclusions

A novel carbon-titania composite material C/$TiO_2$ that can be utilized as a catalyst support has been prepared by decomposition of methane over $TiO_2$ surface using Ni-Cu as a catalyst. The carbon in Pd/C/$TiO_2$ catalyst is composed of nearly 95% of CNFs and 5% of amorphous carbon. And 97% of its textural structures are mesopores. The catalyst Pd/C/$TiO_2$ exhibited 88% of selectivity to citronellal at citral conversion of 90% in citral hydrogenation, which was much higher than that of activated carbon supported Pd catalyst (35%). This was attributed to elimination of internal diffusion limitations, which was significant in activated carbon supported Pd catalyst, due to its microporous structure.

## References

1 Vilella, I. M. J.; De Miguel, S. R.; Salinas-Martínez, L. C.; Linares-Solano, Á.; Scelza, O. A. *Appl*. *Catal*. *A*: *Gen*. **2005**, *281*, 247.
2 Singh, U. K.; Vannice, M. A. *J*. *Catal*. **2001**, *199*, 73.
3 Álvarez-Rodríguez, J.; Cerro-Alarcón, M.; Guerrero-Ruiz, A.; Rodríguez-Ramos, I.; Arcoya, A. *Appl*. *Catal*. *A*: *Gen*. **2008**, *348*, 241.
4 Kiwi-Minsker, L.; Yuranov, I.; Holler, V.; Renken, A. *Chem*. *Eng*. *Sci*. **1999**, *54*, 4785.
5 Li, C. J.; Ma, B. X.; Huo, X. X. *New*. *Carbon*. *Mater*. **1999**, *14*, 19 (in Chinese).
6 Salmi, T.; Mäki-Arvela, P.; Toukoniitty, E.; Neyestanaki, A. K.; Tiainen, L. P.; Lindfors, L. E.; Sjöholm, R.; Laine, E. *Appl*. *Catal*. *A*: *Gen*. **2000**, *196*, 93.
7 Aramendia, M. A.; Borau, V.; Jimenez, C.; Marinas, J. M.; Porras, A.; Urbano, F. J. *J*. *Catal*. **1977**, *172*, 46.
8 Trasarti, A. F.; Marchi, A. J.; Apesteguía, C. R. *J*. *Catal*. **2004**, *224*, 484.
9 Singh, U. K.; Sysak, M. N.; Vannice, M. A. *J*. *Catal*. **2000**,

© 2011 SIOC, CAS, Shanghai, & WILEY-VCH Verlag GmbH & Co. KGaA, Weinheim

*191*, 181.

10 Arvela, P. M.; Tiainen, L. P.; Neyestanaki, A. K.; Sjöholm, R.; Rantakylä, T. K.; Laine, E.; Salmi, T.; Murzin, D. Y. *Appl*. *Catal*. *A*: *Gen*. **2002**, *237*, 181.

11 Aumo, J.; Wärnå, J.; Salmi, T.; Murzin, D. Y. *Chem*. *Eng*. *Sci*. **2006**, *61*, 814.

12 Yilmaz, S.; Ucar, S.; Artok, L.; Gulec, H. *Appl*. *Catal*. *A*: *Gen*. **2005**, *287*, 261.

13 Zhang, Y. J.; Li, J. Y.; Li, W. Z.; Xin, Q. *Chem*. *J*. *Chin*. *Univ*. **2005**, *26*, 1345 (in Chinese).

14 Malathi, R.; Viswanath, R. P. *Appl*. *Catal*. *A*: *Gen*. **2001**, *208*, 323.

15 Mäki-Arvela, P.; Tiainen, L. P.; Lindblad, M.; Demirkan, K.; Kumar, N.; Sjöholm, R.; Ollonqvist, T.; Väyrynen, J.; Salmi, T.; Murzin, D. Y. *Appl*. *Catal*. *A*: *Gen*. **2003**, *241*, 271.

16 Chen, Q. F.; Shi, W. M.; Jiang, D.; Xu, Y.; Wu, D.; Sun, Y. H. *Acta Chim. Sinica* **2010**, *68*, 301 (in Chinese).

17 Wu, J. M.; Yao, J. J.; Yang, H. P.; Fan, Y. N.; Xu, B. L. *Acta Chim. Sinica* **2010**, *68*, 1349 (in Chinese).

18 Wu, F.; Zhu, J.; Li, M. S.; Zhu, J. J.; Shan, Y. H. *Fine*. *Chem*. **2009**, *26*, 561 (in Chinese).

19 Tsoufis, T.; Xidas, P.; Jankovic, L.; Gournis, D.; Saranti, A.; Bakas, T.; Karakassides, M. A. *Diam*. *Relat*. *Mater*. **2007**, *16*, 155.

20 Delbecq, F.; Sautet, P. *J*. *Catal*. **1995**, *152*, 217.

(E1009141 Sun, H.; Fan, Y.)